Soil-structure interaction analysis in reinforced concrete structures on footing foundation

Yago Ryan Pinheiro dos Santos[1]# iD, Maria Isabela Marques da Cunha Vieira Bello[1] iD,

Alexandre Duarte Gusmão[2] iD, Jonny Dantas Patricio[3] iD

Article

Abstract

Soil-structure interaction (SSI) evaluates how soil or rock deformability imposes on the structure a different load path in a hypothesis of fixed supports, altering the loads acting on the structural elements and the ground. This paper discusses the results of the SSI effects in two buildings with a reinforced concrete structure and shallow foundations in a rock mass. The settlements were monitored by field instrumentation in five stages of their construction, making it possible to estimate through interpolation curves the settlements values of some points. The numerical modeling and structural analysis of the buildings were obtained for two different cases of soil-structure interaction. The structure was considered having fixed supports (non-displaceable) and displaceable supports (with stiffness spring coefficients K). The results reveals the occurrence of SSI effects, with a load redistribution between the columns that occurred differently for the different construction stages. Structural modeling proved to be quite representative, pointing to higher vertical load values than the average values present in building edge zones, which contradicts the conventional idea that central columns are more loaded than the edge columns. The soil-structure interaction analyses resulted in different behaviors regarding both towers; pointing out that low settlements and building symmetry in plan minimize the effects of interaction, with no tendency of load redistribution between columns as the structure rigidity increases, as construction development.

1. Introduction

Reinforced concrete structure projects are elaborated usually considering three distinct parts: the superstructure, composed of slabs, beams, and columns; the infrastructure, consisting of the foundation elements (shallow or deep), and finally, soil or rock mass, which support the requests coming from superstructure. The interaction between these parts is the soil-structure interaction (SSI), whose mechanism describes the structural system performance.

The principal consideration of SSI studies in buildings is the adoption of flexible supports. The conventional approaches to determine settlement has been estimated based on elastic theory.

Shallow spread footings are generally designed as foundations at rock sites (Chaudhary, 2016). Individual footing foundation settlement analysis usually assumed the soil/rock to consist of independent linear springs (Winkler's hypothesis) or uses Elastic Continuum Method (Winkler, 1867).

Meyerhof (1953), Morris (1966), Lee & Brown (1972), and Poulos (1975) proposed SSI analysis. Factors such as floor numbers, construction processes and sequence, building shape and other effects related to soil/rock and structure behavior, contribute to the mechanisms of this mutual influence (Gusmão, 1994).

Danziger et al. (2005), Mota (2009), Savaris et al. (2011), Santos (2016) analyzed real cases of buildings through monitored settlements. The settlements measurement along different construction stages enables to observe loads redistribution between central and the edge reinforced concrete columns. In general, there was a tendency of load relief in the central column and overload the edge column, after considerations of SSI; Rosa et al. (2018) also point out that the greater load and settlement redistribution are usually observed more effectively at the beginning of construction, when the building structure stiffness tends to increase until the first floors.

#Corresponding author. E-mail address: yago_ryan@hotmail.com
[1]Universidade Federal de Pernambuco, Departamento de Engenharia Civil, Caruaru, PE, Brasil.
[2]Universidade de Pernambuco, Departamento de Engenharia, Recife, PE, Brasil.
[3]Universidade Federal de Campina Grande, Departamento de Engenharia Civil, Campina Grande, PB, Brasil.

Santos & Corrêa (2018) also assessed load redistribution caused by SSI among foundations elements in a building with concrete walls by means of iterative numerical analyses, and observed a tendency of load transfer to supports under greater settlements to supports with lower settlements, and finally a uniformity of settlements among columns.

Other analyses, such as the dynamic effects of vibrations and seismicity combined with soil-structure interaction in buildings (Papadopoulos et al., 2017; Amini et al., 2018; Gómez-Martínez et al., 2020) point to the idea that the SSI mechanisms play a considerable role on behavior of buildings, directly influencing the propagation of vibrations throughout the structural elements; therefore, the consideration of SSI is extremely important for controlling the performance of structures when subjected to these events.

Considering the importance of the subject concerning economic, safety, performance and durability factors, the present paper has the objective to contribute to the study of soil-structure interaction by the analysis of the SSI effects to represent the behavior of a reinforced concrete structure with spread footings foundation.

2. Characterization of the study area

The study considered two residential buildings with reinforced concrete frame structures, called "tower A" and "tower B", located in Caruaru, Pernambuco, Brazil. Tower A is 32-floor and tower B is 35-floor. The geological-geotechnical investigation comprised 14 boreholes performed by rotary-percussion drilling. The ground boreholes at tower A location reached depths between 5.27 m and 11.30 m, with a light-colored shallow soil layer composed of sand and gravel, followed by a light-colored altered rock layer. The tower B boreholes have depths between 3.80 m and 10.80 m, with

a superficial layer of a sandy embankment and light sandy soil with gravels, followed by altered light-colored rock.

Cataclastic metamorphic rock was observed on depths between 0.40 m and 11.30 m the Tower A location, and between 0.50 m and 10.80 m on the Tower B location. The Rock Quality Designation (RQD) values were higher than 75%, being classified as a good to excellent recovery RQD, and absence of water table. Figures 1a and 1b show the representative geotechnical profile of towers A and B, respectively. Unconfined compressive strength test was performed on eight cylindrical rock samples with dimensions of 5.4 cm × 10.8 cm (diameter × height), extracted from different depths of drilling. The samples presented unconfined compression strength (UCS) between 83.0 MPa and 175.0 MPa, with an average value of 110.90 MPa, a standard deviation of 33.13 MPa, and a coefficient of variation (COV) of 30%.

Figure 2 shows the foundation plan of towers A and B, and the location of their respective boreholes. Due to the ground characteristics, shallow spread and combined footings foundation. All footings were designed for allowable pressure of 1040 kPa for the case where it considers the combination of permanent loads and wind action.

3. Field instrumentation for building settlements monitoring

The settlements were monitored during buildings construction by field instrumentation. Ten topographic monitoring bolts were installed on all 22 and 18 columns located on the ground floor of towers A and B, respectively. Readings were taken at five different construction stages. The first reading was taken when bolts were installed (reading 0), and the last reading was performed at a stage near to the construction end. Table 1 shows the construction stages of towers A and B at the time of the readings.
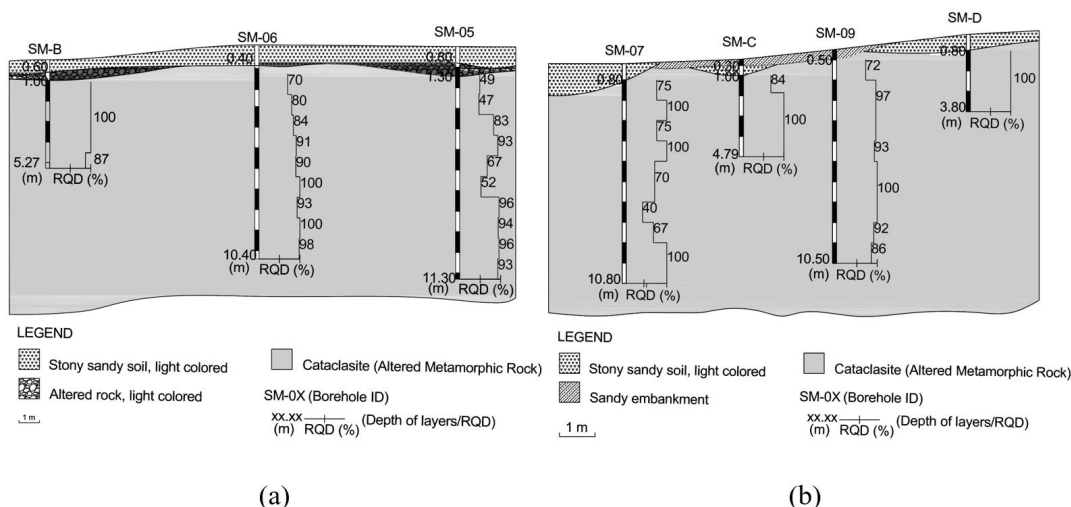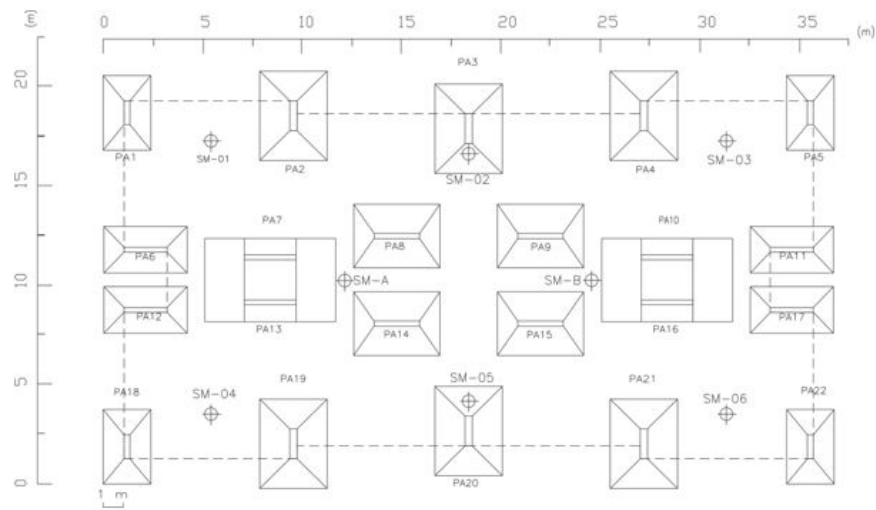

Figure 1. Representative geotechnical underground profiles: towers (a) A and (b) B.

(a)
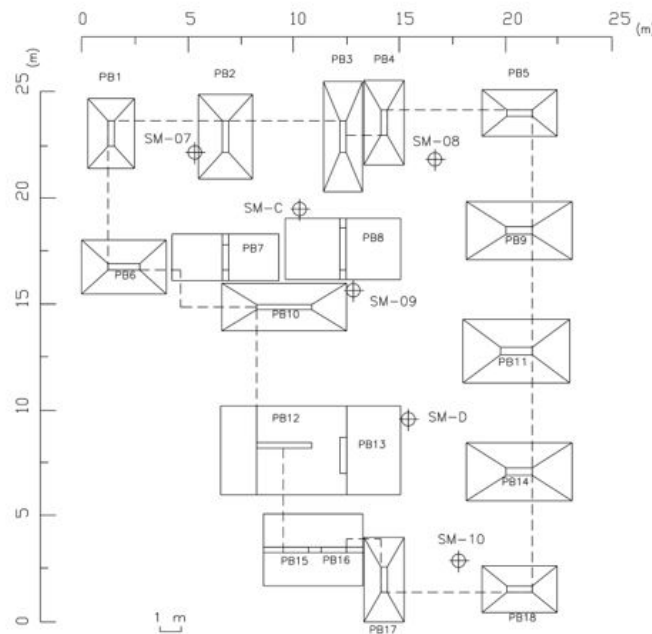
(b)

Figure 2. Location of the rotary-percussion drilling and plan of the shallow foundation: (a) tower A and (b) tower B.

Table 1. Construction stages of towers A and B.

Reading n.		0	1	2	3	4
Time passed (days)		0	265	355	530	708
Stage	TOWER A	ground floor slab	7th floor type subfloor	5th floor-type inner wall cladding	5th floor-type external wall cladding	32th floor-type ceiling
	TOWER B	ground floor slab	1st floor-type inner wall cladding	9th floor-type inner wall cladding	5th floor-type ceiling	34th floor-type ceiling

4. Structural modeling of buildings

The structural model of both buildings was constructed using TQS software® (TQS, 2021) considering initially fixed supports (non-displaceable) to determine the support reactions in each stage of the construction of tower A and B (Table 2 and 3, respectively). After, the support reactions were related to monitored settlement to determine spring coefficients K. Two analyses of the support springs was done of soil-structure interaction, called SSI 1 and SSI 2.

In SSI 1 analysis, spring coefficients at the different construction stages (K_i) were obtained by the ratio of the vertical support reaction (Fz_i) to the monitored settlement by each support (δ_i) (Equation 1). The average spring coefficient of the structural supports for each construction stage (K_m) was determined in SSI 2 analysis. This coefficient was obtained by the ratio of the vertical support reaction average of the structure for each construction stage (Fz_m) to the average monitored settlement δ_m (Equation 2).

$$K_i = \frac{Fz_i}{\delta_i}(kN/m) \tag{1}$$

$$K_m = \frac{Fz_m}{\delta_m}(kN/m) \tag{2}$$

For each monitored settlement reading, the elastic supports of the structure had an associated K value that was fed into the TQS software® for both analyses, corresponding to each foundation element. Then, the superstructure will respond according to the SSI mechanisms, with its flexible supports, obtaining values of resulting loads after interaction.

5. Results and discussion

Results of settlement estimation, analysis of soil-structure interaction considering foundation on rock are presented and discussed.

5.1 Buildings settlement analysis

Figure 3a and 3b show the settlements evolution with time of tower A and B, respectively.

Settlement readings no. 1, 2, and 3 of tower A shows the greatest deformations are observed around the PA20 column, where the highest settlements of these readings were recorded (9.84 mm, 14.48 mm and 18.37 mm). The settlement reading no. 4 showed the greatest deformation in lower right portion of the ground, which was observed surrounding PA21 column (17.38 mm). Settlement reduction for PA20 in stage 4 may be related to some reading error during monitoring; however, it was decided to proceed the analysis with this value.

Analyzing the tower B, readings no. 1, 2 and 3 show a more significant deformation surrounding PB03 and PB04 (upper edge) and PB11 (right edge), where settlement

Table 2. Support reactions (loads) of tower A.

Column	Support reactions - loads (kN)			
	Stage 1	Stage 2	Stage 3	Stage 4
PA01	3072.49	4462.57	5922.30	6897.41
PA02	5229.71	7731.26	10285.79	11755.32
PA03	5283.67	7935.31	10783.15	12461.64
PA04	5202.24	7649.84	10168.07	11623.87
PA05	3049.93	4266.37	5634.86	6564.85
PA06	3035.21	4543.99	6147.93	7036.71
PA07	4112.35	6679.63	9151.75	10129.81
PA08	4842.22	7809.74	10889.10	12076.11
PA09	4574.4	7125.00	10083.70	11196.15
PA10	3941.66	6184.22	8525.87	9422.51
PA11	3239.26	4905.98	6759.09	7711.64
PA12	3202.97	4746.08	6389.25	7293.74
PA13	4431.18	7091.65	9675.60	10695.84
PA14	4937.37	7929.42	10741.95	11870.10
PA15	4725.48	7369.27	10059.17	11077.45
PA16	3693.47	5707.46	7825.44	8619.07
PA17	3705.24	5521.07	7515.44	8549.42
PA18	3332.46	4853.01	6279.38	7268.23
PA19	5937.99	8721.09	11351.15	12894.26
PA20	5727.08	8491.54	11245.20	12856.99
PA21	5822.24	8580.81	11205.96	12743.19
PA22	3482.55	4952.09	6325.49	7288.83
TOTAL	94581.20	143257.40	192965.60	218033.10

Table 3. Support reactions (loads) of tower B.

Column	Support reactions - loads (kN)			
	Stage 1	Stage 2	Stage 3	Stage 4
PB01	2923.38	3804.32	4662.69	5307.21
PB02	4331.12	6031.19	7449.71	8408.15
PB03	3808.24	5365.09	6154.79	6839.53
PB04	3152.93	4483.17	5468.09	6262.70
PB05	2849.81	3883.78	4531.24	5155.16
PB06	3184.33	4370.36	5289.55	6024.32
PB07	4131.97	6148.91	7646.90	8505.27
PB08	6144.98	8799.57	11448.27	12435.16
PB09	4993.29	7182.88	8968.30	10159.24
PB10	3901.44	5420.03	6277.42	7014.15
PB11	7087.73	10429.01	12049.62	13207.20
PB12	3985.80	5954.67	7119.12	8086.38
PB13	8035.37	14353.01	13143.44	13894.88
PB14	5640.75	8458.18	9716.81	10981.31
PB15	1552.92	2279.84	1672.61	1753.05
PB16	6427.51	9999.33	8629.86	8932.01
PB17	2725.22	6367.67	4679.37	5321.93
PB18	2735.03	3878.87	4269.31	4897.15
TOTAL	77611.82	117209.88	129177.10	143184.80
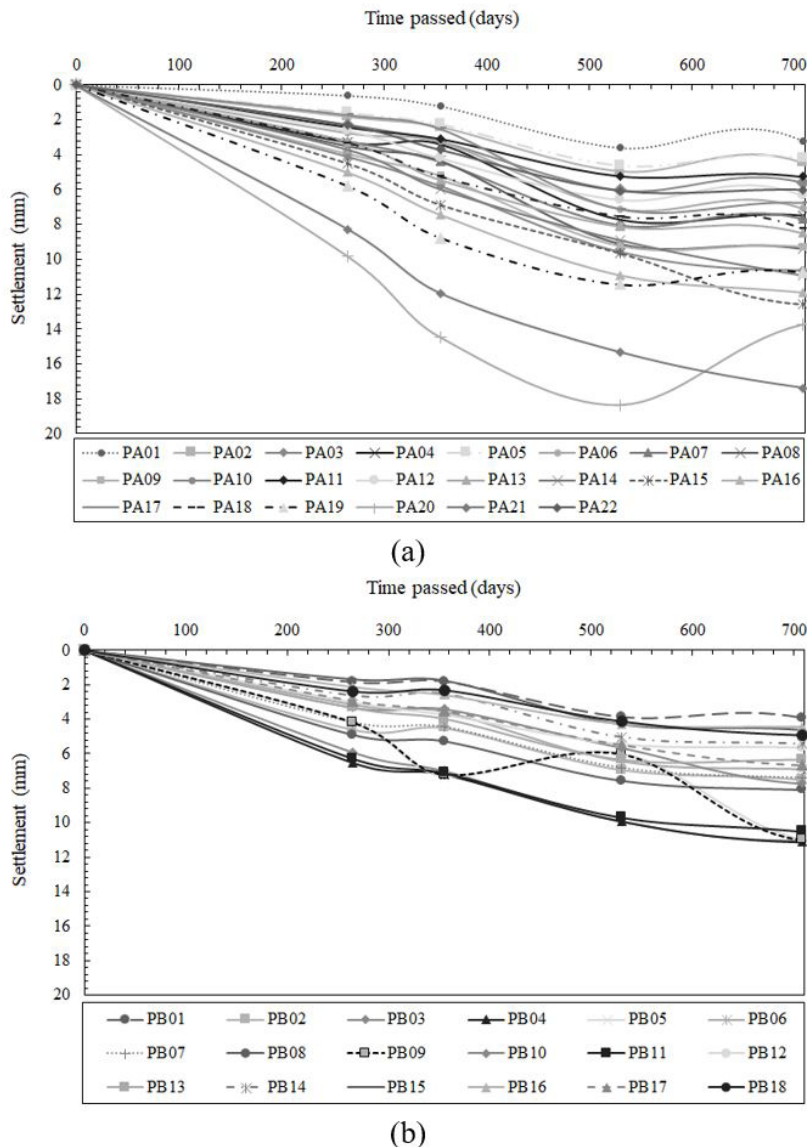
Figure 3. Settlement evolution with the observed time: (a) tower A; (b) tower B.

values were 5.90 mm, 6.51 mm and 6.27 mm in reading no. 1, 6.98 mm, 7.18 mm and 7.10 mm in reading no. 2 and 9.90 mm, 9.91 mm and 9.69 mm in reading no. 3 in this order, respectively. The settlement of reading no. 4 has the highest settlement surrounding PB03, PB04 and PB05 (11.02 mm, 11.11 mm and 11.00 mm, respectively), and surrounding PB09 (11.00 mm) and PB11 (10.50 mm). Note that the most significant settlements were maintained at all stages in PB04 column and similarly in PB11 column. PA21 and PA01 of tower A presented the highest and lowest final absolute settlements (17.38 mm and 3.20 mm, respectively); PB04 and PB01 of tower B presented the highest and lowest final absolute settlements (11.11 mm and 3.92 mm, respectively).

Figures 4 and 5 shows settlement isolines and 3D representation of settlement for the ground of tower A and B, respectively, in stage 3.

A tendency of the highest measured settlement was observed to occur in the lower edge of the foundation of both towers A and B, differing from what commonly happens, which is higher settlement in the central region of building, reported by Gusmão (1994). This fact can be attributed to the geomechanical conditions of the subsoil and to fact that the loads resulting from the columns are larger in this area, which causes larger ground deformations.

5.2 Analysis of the soil-structure interaction

Figure 6 and Figure 7 show examples of force redistribution on the foundation between the columns of tower A and B, respectively, in which the painted areas refer to force increase and the blank areas refer to force reduction in the columns.

The redistribution of forces observed is distinct for SSI 1 analysis. While for SSI 2, this redistribution is more
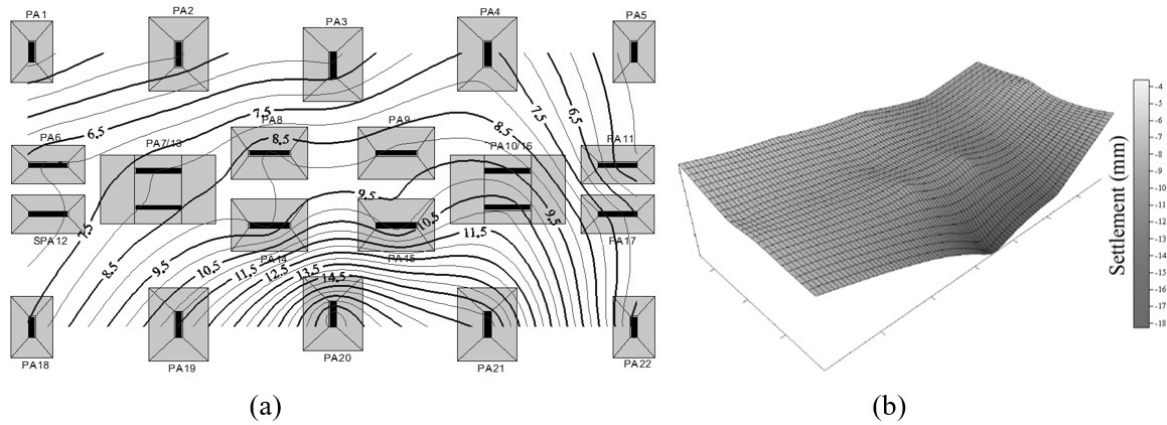
(a)

(b)

Figure 4. (a) Settlement isolines curves and (b) shape of ground surface settlement of tower A – Stage 3.
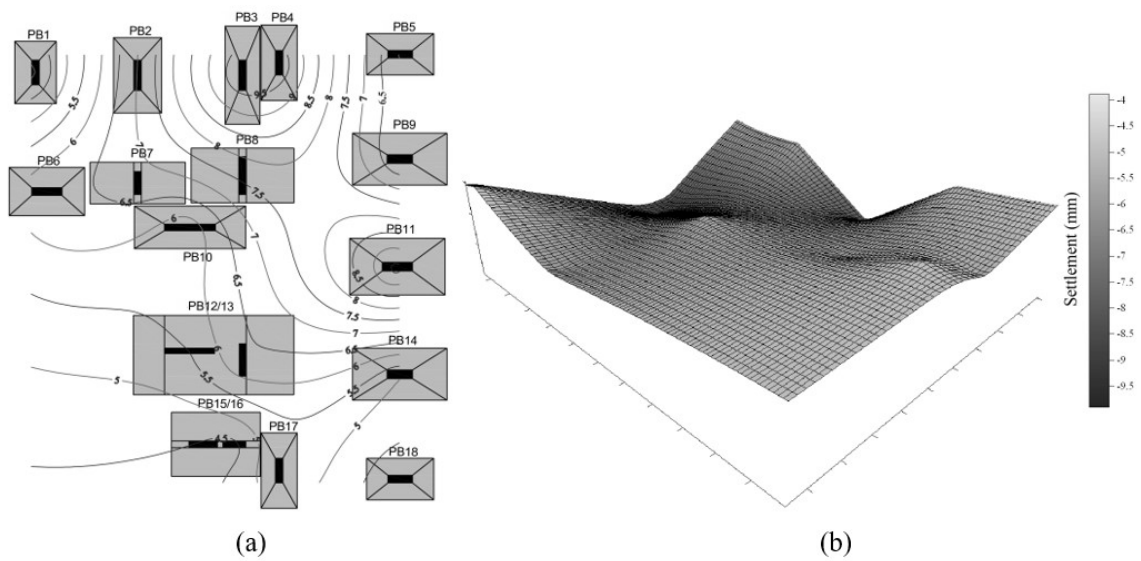

(a)

(b)

Figure 5. (a) Settlement isolines curves and (b) shape of ground surface settlement of tower B – Stage 3.
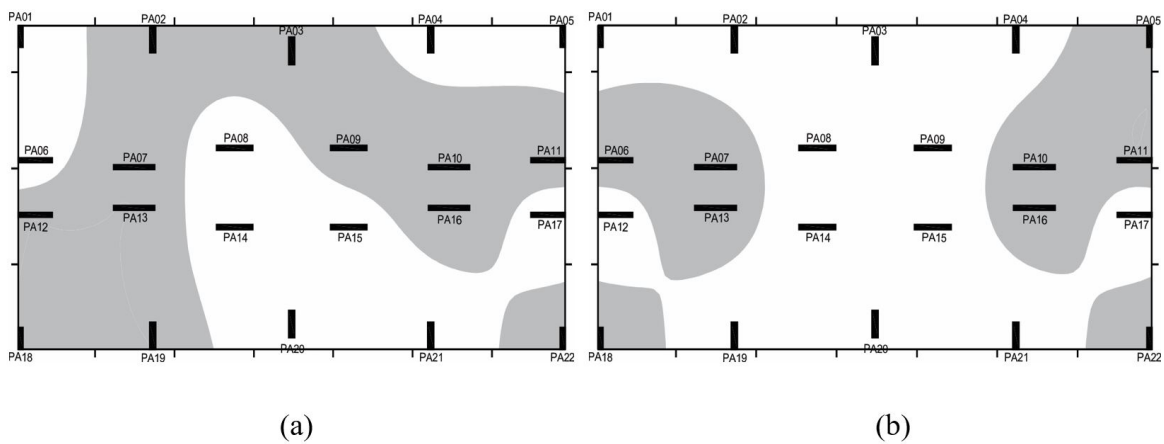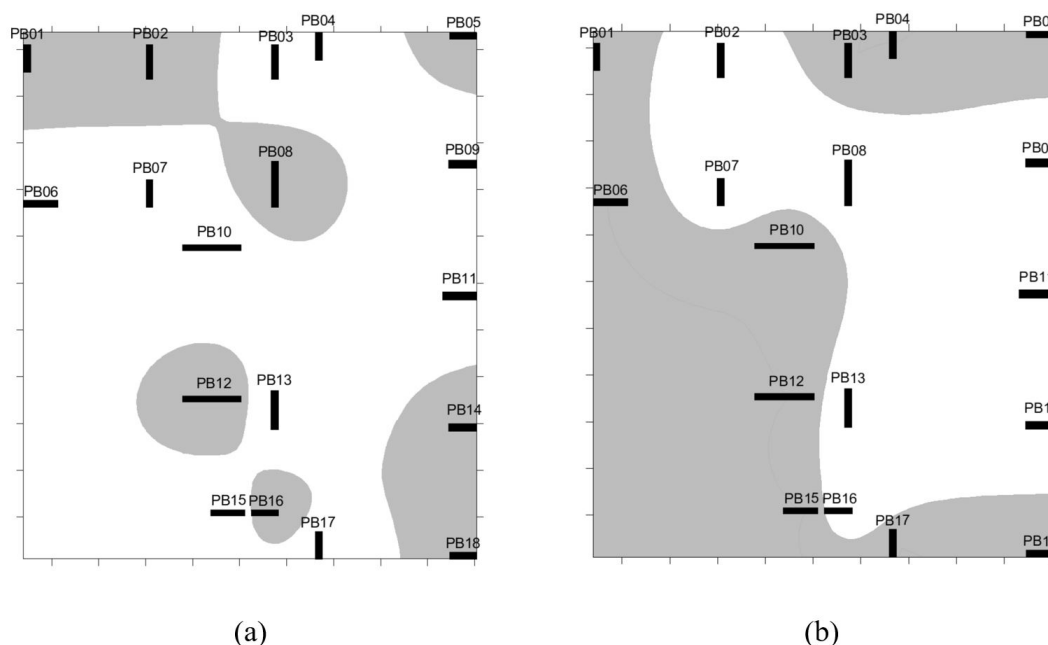

(a)

(b)

Figure 6. Efforts redistribution in plant between the columns of tower A in (a) SSI case 1 and (b) SSI case 2 - stage 4.

Figure 7. Efforts redistribution in plant between the columns of tower B in (a) SSI 1 and (b) SSI 2 - stage 4.

Table 4. Redistribution of total efforts in percentage (%) - towers A and B.

Stage	Redistribution (%)							
	Central columns				Edge columns			
	Tower A		Tower B		Tower A		Tower B	
	SSI 1	SSI 2	SSI 1	SSI 2	SSI 1	SSI 2	SSI 1	SSI 2
1	-0.67	-0.66	-1.32	-10.07	1.10	0.88	0.37	3.07
2	-0.72	-0.55	-0.68	-12.01	1.08	0.67	0.17	3.97
3	-0.51	-0.51	-1.55	-11.81	0.63	0.55	0.47	3.89
4	0.09	-0.57	0.11	-11.93	-0.25	0.68	-0.10	3.79

subtle, presenting the same behavior in stages 2, 3 and 4, in which the same columns are relieved and overloaded. This phenomenon can be explained by the fact that the adoption of the K_m spring coefficient is determined by the average loading and the average settlement of the building columns, where each support has a dislocation with the same rigidity. This makes the SSI behavior more uniform, reducing even more the rock mass variability, thus generating very similar results.

Table 4 shows loads redistribution, through the rate of load gain or loss of towers columns. Considering tower A, in SSI 1 and SSI 2 analysis, there was variation in load redistribution behavior between its columns. In terms of total efforts, stages 1, 2, and 3 showed the expected behavior for the column's redistribution considering the SSI, in which the central columns are relieved, and the edge columns show a load increase.

In SS1 and SSI 2 analyses considering the tower B, the most significant load relief in the central columns and the highest load gain in the edge columns in terms of total forces was observed at the construction stage 3 (-1.55% and 0.47%, respectively). For SSI 2, all construction stages behaved as expected. The greatest relief of total forces in

the central columns occurred at stage 2 (-12.01%), as well as the greatest total force gain in the edge columns, with a value of 3.97%. Comparing the towers, the redistribution of total forces between central and edge columns is slightly more expressive in SSI 2. Stage 4 behaved contrary to the previous stages considering the SS1 analysis in both towers, which may be associated with the amount of total forces that was redistributed at a given stage.

Figure 8 and Figure 9 relate, respectively for towers A and B, the percentage of central columns that undergo stress-relief and the number of edge columns that experienced an increase of forces in function of the construction stage. In SSI 1 analysis, a total of 4 central columns of tower A experienced force relief (50%), in stages 1 and 3.

Regarding the increase of forces in the edge columns, the redistribution was more significant in construction stages 2 and 3, where 7 columns (50%) were overloaded after the analysis. For the SSI 2 analysis, 35.70% of the edge columns exhibited gain of forces during all construction stages. This behavior was similar to the central columns, where, until stage 4, 50% of the columns showed load relief. For tower B, in SSI 1 analysis, a total of 2 central columns underwent
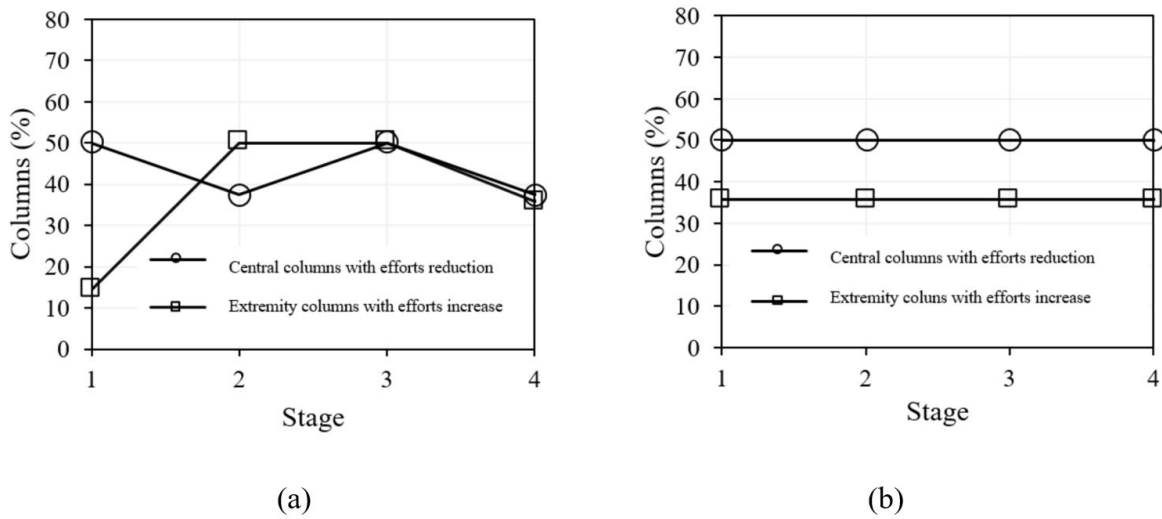
Figure 8. Central columns with reduction and edge columns with efforts increase of tower A: (a) SSI case 1; (b) SSI case 2.
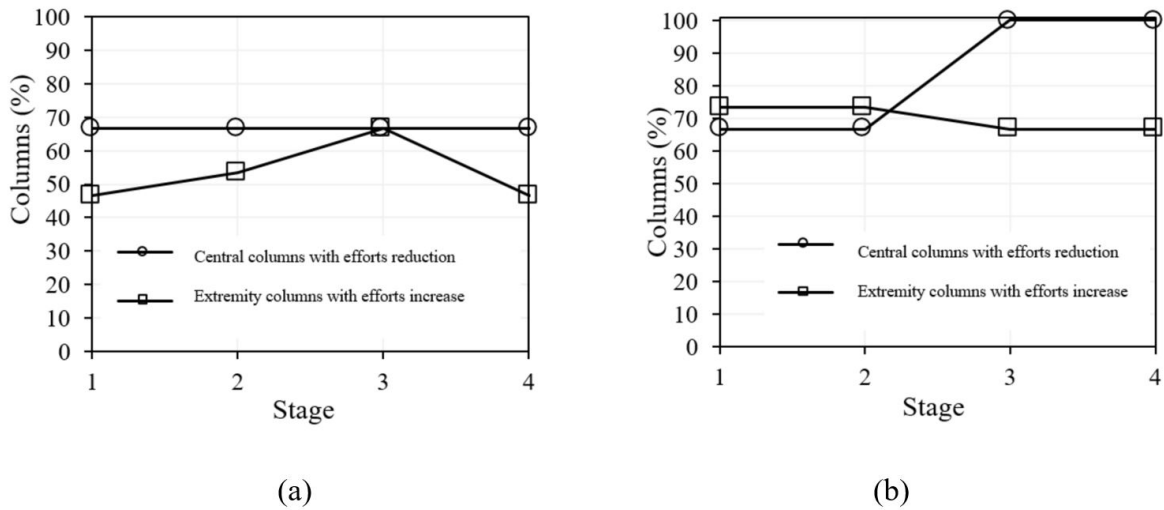

Figure 9. Central columns with reduction and end edge columns with efforts increase of tower B: (a) SSI case 1; (b) SSI case 2.

to effort relief (66.67%). Regarding the edge columns, the force gain was more significant in stage 3, in which 66.67% (10 edge columns) experienced this type of redistribution. In SSI 2 analysis, 66.67% of the total central columns presented load relief for the other stages. The edge columns showed an increase in forces of 73.33% (11 columns) in stages 1 and 2, reducing this ratio to 66.67% in other stages (10 columns).

This behavior shows the phenomenon of load redistribution in the columns related to the SSI, with a load relief of the central columns and overload of the edge columns. It should also be noted that not all central and edge columns, in most observed construction stages, were relieved and overloaded, respectively. Danziger et al. (2005) and Santos (2016) also noted this fact.

The following analysis consists of evaluating the redistribution of forces between the columns considering the settlement experienced by them. Therefore, considering the average settlement observed for each of the construction stages, it was

possible to determine the columns that experienced settlement superior and inferior to the average value. This happened because the tendency is that the columns that present settlement above the average are the most loaded ones, and those with settlement lower than the average are the least loaded. Then, after the SSI, it is expected stress relief on columns with the above average settlement and stress gain on columns that have below-average settlement, considering that the most loaded ones are not in center but at the edge. Figure 10 and Figure 11 show the number of columns that have been relieved and those that experienced force increase after the soil-structure interaction (cases 1 and 2) for the buildings, considering this analysis.

Considering tower A for the SSI 1 analysis (Figure 10a), the largest reduction in efforts of them occurred in stage no. 1, in 91.70% of the columns. Concerning the number of columns that had load increase, this gain was more significant in stage 4 (61.50%).

Analyzing the results obtained through SSI 2 (Figure 10b), the force reduction between the columns that presented higher settlement than the average was more significant in stages 3 and 4, with 77.80% of these columns that suffered such redistribution and being less expressively in stage 2.

In tower B, during SSI 1 (Figure 11a), the reduction of efforts between the columns that presented settlement higher than the average is more expressive in stage 3, where 75% of these columns were relieved. Concerning the increase of efforts between the columns that presented settlement lower than the observed average, the stage 3 is also the one with the most significant amount, where 90% of these columns gain some load with the SSI. Considering SSI 2 (Figure 11b), the tower presented the largest number of columns with settlement larger than the observed average, and that suffered a reduction of its efforts in stage 3, which relief occurred in 50% of these elements. The force gain in the columns with lower settlements than the average was more expressive in stages 1, 2, and 3, which 70% of these columns were more overload than the analysis without the interaction. Figure 12 and Figure 13 represent the force redistribution in terms of reduction and increase of maximum forces, for the construction stages of towers A and B, respectively.

In both analyses, force relief and gain are observed as the construction nears completion. In tower A, concerning the SSI 1 analysis, the greatest force gain was noted in PA22 in stages 3 and 4, and the greatest force relief in PA20, in stage 2. As for SSI 2 analysis, the PA16 was the one that obtained the greatest efforts gain in stages 3 and 4. The greatest effort relief was observed in PA08 in stage 3.

In tower B, for SSI 1 analysis, the greatest force gain was observed in PB15 (24.83%) at stage 2, and the greatest stress relief in PB17 at construction stage 4. According to the SSI 2 analysis, the largest increase was observed in PB15 at stage 4 (Figure 13b), while the most significant reduction was observed in stage 1, in PB16 (Figure 13b). Such variation may be attributed to the asymmetry of the building plan, making the redistribution not to be observed in a more uniform and less accentuated way as observed between the columns of tower A.

Figures 14a and 14b represent the redistribution, in average terms, of the column forces in towers A and B, respectively, in SSI 1 and SSI 2 analyses. This figure shows that the average force redistribution occurred between the columns that were relieved and that gained load after the soil-structure interaction, for the analyzed construction stages.
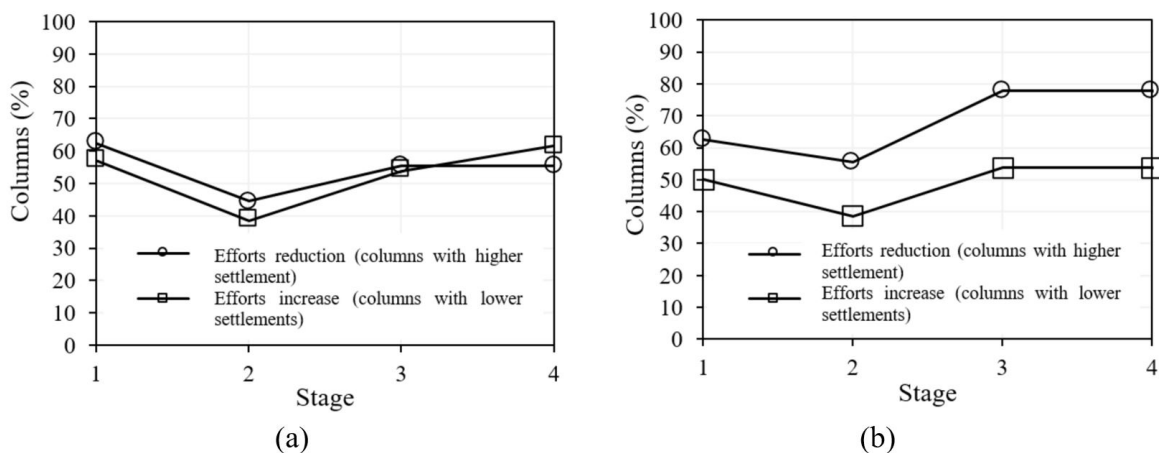

(a)   (b)

Figure 10. Columns with force reduction (higher settlement) and increase (lower settlements) in tower A: (a) SSI 1; (b) SSI 2.
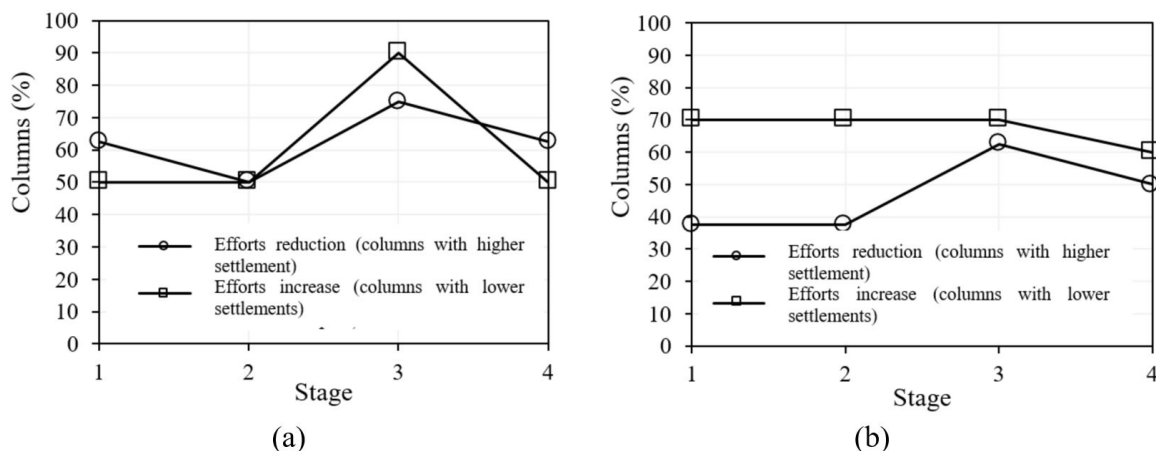

(a)   (b)

Figure 11. Columns with force reduction (higher settlement) and increase (lower settlements) in tower B: (a) SSI 1; (b) SSI 2.
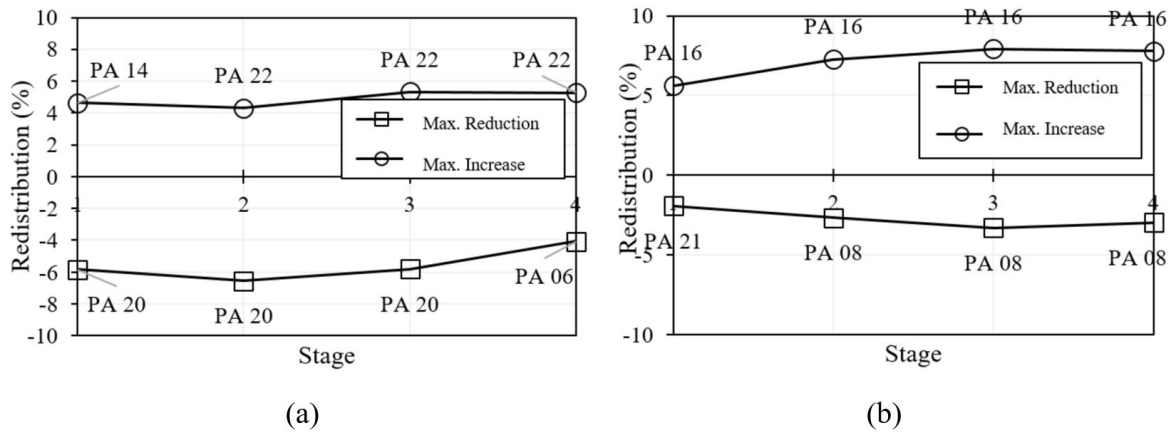
(a)

(b)

Figure 12. Force redistribution in terms of reduction and a maximum increase of tower A: (a) SSI case 1; (b) SSI case 2.
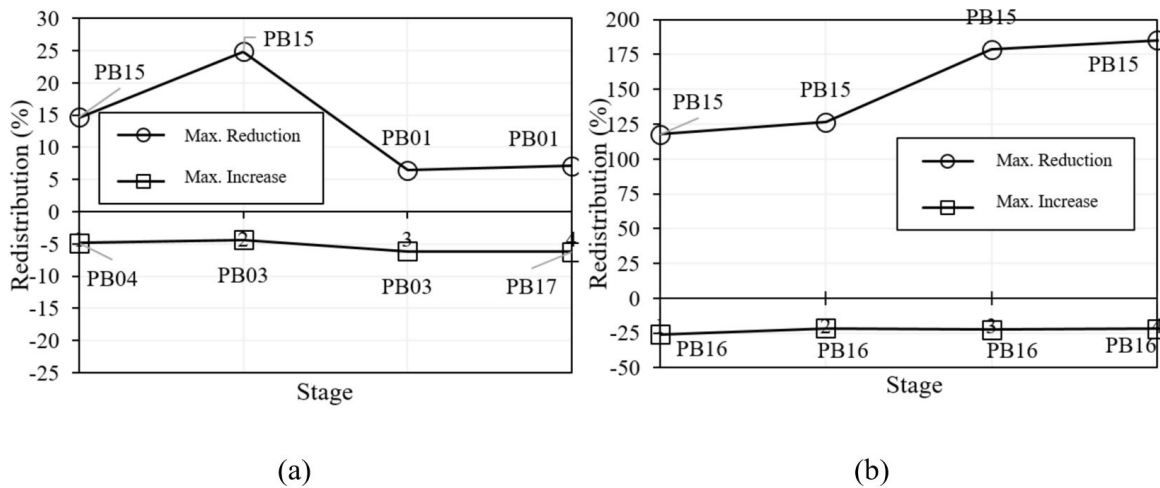

(a)

(b)

Figure 13. Force redistribution in terms of reduction and a maximum increase of tower B: (a) SSI case 1; (b) SSI case 2.
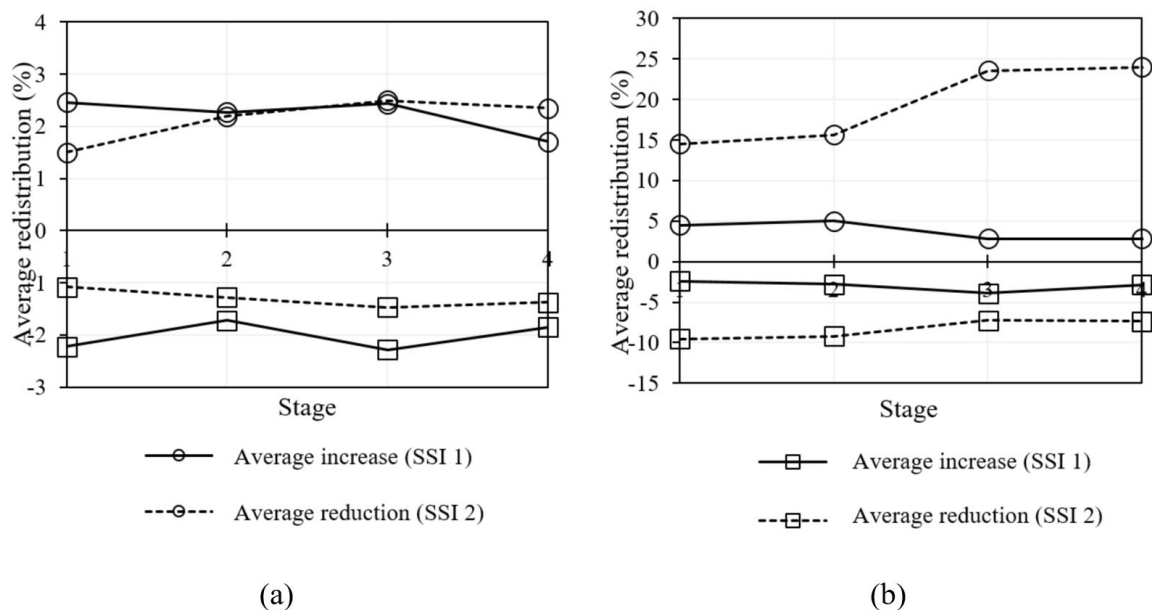

(a)

(b)

Figure 14. Force redistribution between the columns in average terms: (a) tower A; (b) tower B.

It was not possible to notice a tendency to reduce the force redistribution between the columns as the construction comes to its conclusion (the increase of the structure rigidity) as stated by Gusmão (1994) and Santos (2016). This can be attributed to low settlement values and symmetry in plan observed in tower A, and low settlement values of tower B, thus minimizing the SSI effects.

6. Conclusions

The structural modeling proved to be quite representative, pointing to vertical load values higher than the average values present in building edge zones, contradicting the conventional idea that the central columns are more loaded than the edge columns.

The soil-structure interaction analyses resulted in different behaviors regarding both towers, construction stages, and SSI 1 and SSI 2 analyses. Redistribution values were lower in tower A compared to tower B. This fact can be explained by the asymmetry in plan of tower B projection, differing from the plan projection of tower A, which is symmetrical, and thereby, has a smaller redistribution, varying slightly from its efforts when non-displaceable structure is considered. There was no decreasing trend in force redistribution between the columns of both towers as the construction was near to the conclusion (the increase of the structure rigidity). The phenomenon behaved quite distinctly between the stages.

Analyses that include maximum values of force reduction and gain, as well as those that demonstrate redistribution by relating the settlement magnitude, give a more complete and comprehensive view of the phenomena attributed to the SSI.

Acknowledgements

Declaration of interest

There is no conflicting interests.

Author's contributions

Yago Ryan Pinheiro dos Santos: data curation, conceptualization, methodology, validation, writing - original draft preparation. Maria Isabela Marques da Cunha Vieira Bello: validation, supervision, writing - reviewing and editing. Alexandre Duarte Gusmão: data curation, validation, supervision. Jonny Dantas Patricio: supervision, writing - reviewing and editing.

List of symbols

Fz_i	Vertical Support Reaction
Fz_m	Vertical Support Reaction Average
K	Spring Coefficient
K_i	Spring Coefficient at the Different Construction Stages
K_m	Average Spring Coefficient
RQD	Rock Quality Designation
SSI	Soil-Structure Interaction
UCS	Unconfined Compressive Strength
δ_i	Monitored Settlement
δ_m	Average Monitored Settlement

References

Amini, F., Bitaraf, M., Nasab, M.S.E., & Javidan, M.M. (2018). Impacts of soil-structure interaction on the structural control of nonlinear systems using adaptive control approach. *Engineering Structures*, 157, 1-13. http://dx.doi.org/10.1016/j.engstruct.2017.11.071.

Chaudhary, M.T.A. (2016). Effect of soil-foundation-structure interaction and pier column non-linearity on seismic response of bridges supported on shallow foundations. *Australian Journal of Structural Engineering*, 17(1), 67-86. http://dx.doi.org/10.1080/13287982.2015.1116178.

Danziger, B.R., Carvalho, E.M.L., Costa, R.V., & Danziger, F.A.B. (2005). Case study with soil-structure interaction analysis. *Civil Engineering Magazine*, 23, 43-54.

Gómez-Martínez, F., Millen, M.D.L., Costa, P.A., & Romão, X. (2020). Estimation of the potential relevance of differential settlements in earthquake-induced liquefaction damage assessment. *Engineering Structures*, 211, 110232. http://dx.doi.org/10.1016/j.engstruct.2020.110232.

Gusmão, A.D. (1994). Relevant aspects of soil-structure interaction in buildings. *Soils and Rocks*, 17(1), 47-55.

Lee, I.K., & Brown, P.T. (1972). Structure-foundation interaction analysis. *Journal of the Structural Division*, 98(11), 2413-2431.

Meyerhof, G.G. (1953). Some recent foundation research and its application to design. *Structural Engineering*, 31, 151-167.

Morris, D. (1966). Interaction of continuous frames and soil media. *Journal of the Structural Division*, 92(5), 13-44. http://dx.doi.org/10.1061/JSDEAG.0001505.

Mota, M.M.C. (2009). *Soil-structure interaction in deep foundation buildings: numerical method and observed field results* [Doctoral thesis]. University of São Paulo (in Portuguese). https://doi.org/10.11606/T.18.2009.tde-15122009-111356

Papadopoulos, M., Van Beeumen, R., François, S., Degrande, G., & Lombaert, G. (2017). Computing the modal characteristics of structures considering soil-structure interaction effects. *Procedia Engineering*, 199, 2414-2419. http://dx.doi.org/10.1016/j.proeng.2017.09.296.

Poulos, H.G. (1975). Settlement analysis of structural foundation systems. In *Proc. 4th Southeast Asian Conference on Soil Engineering* (pp. 52-62), Kuala Lumpur, April 1975. Kuala Lumpur: The Institution.

Rosa, L.M.P., Danziger, B.R., & Carvalho, E.M.L. (2018). Soil-structure interaction analysis considering concrete creep and shrinkage. *Ibracon Structures and Materials Journal*, 11(3), 564-585. http://dx.doi.org/10.1590/S1983-41952018000300008.

Santos, M.G.C., & Corrêa, M.R.S. (2018). Analysis of the effects of soil-structure interaction in reinforced concrete wall buildings on shallow foundation. *Ibracon Structures and Materials Journal*, 11(5), 1076-1109. http://dx.doi.org/10.1590/S1983-41952018000500010.

Santos, M.J.A.P. (2016). *Soil x structure interaction: analysis of a work case with repression monitoring since the beginning of construction* [Master's dissertation]. Rio de Janeiro State University (in Portuguese). Retrieved in April 20, 2021, from http://www.bdtd.uerj.br/handle/1/11641

Santos, Y.R.P. (2018). *Study of the soil-structure interaction of a construction case of rocky mass foundations* [Master's dissertation]. Federal University of Pernambuco (in Portuguese). Retrieved in April 20, 2021, from https://repositorio.ufpe.br/handle/123456789/31862

Savaris, G., Hallak, P.H., & Maia, P.C.A. (2011). Understanding the mechanism of static soil-structure interaction: a case study. *Soils and Rocks*, 34(3), 195-206.

TQS. (2021). *About TQS.* Retrieved in April 20, 2021, from https://www.tqs.com.br/

Winkler, E. (1867). *Die lehre von elasticitaet und festigkeit.* Verlag H. Dominicus (in German).